Nanoscale

Accepted Manuscript

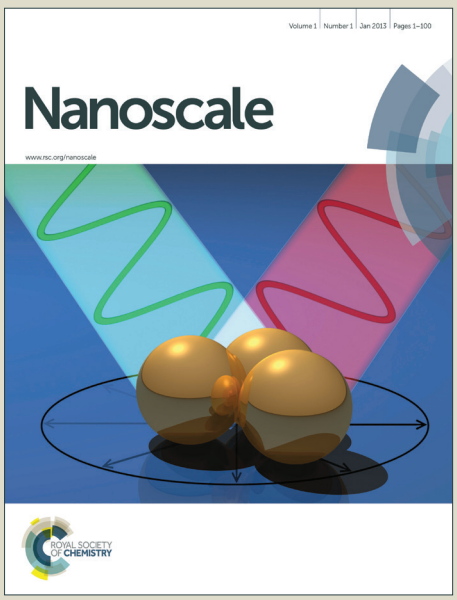

ROYAL SOCIETY OF CHEMISTRY

www.rsc.org/nanoscale

Polypyrrole Nanoparticles for Tunable, pH-Sensitive and Sustained Drug Release

Devleena Samanta[a], Jana L. Meiser[a,b] and Richard N. Zare[a,*]
[a]Department of Chemistry, Stanford University, Stanford, CA, 94305, USA
[b]Leibniz Universität Hannover, 30167 Hannover, Germany

* Corresponding author
email: zare@stanford.edu

Abstract

We report the development of a generalized pH-sensitive drug delivery system that can release any charged drug preferentially at the pH range of interest. Our system is based on polypyrrole nanoparticles (PPy NPs), synthesized via a simple one-step microemulsion technique. These nanoparticles are highly monodisperse, stable in solution over the period of a month, and have good drug loading capacity (~15 wt%). We show that PPy NPs can be tuned to release drugs at both acidic and basic pH by varying the pH, the charge of the drug, as well as by adding small amounts of charged amphiphiles. Moreover, these NPs may be delivered locally by immobilizing them in a hydrogel. Our studies show encapsulation within a calcium alginate hydrogel results in sustained release of the incorporated drug for more than 21 days. Such a nanoparticle-hydrogel composite drug delivery system is promising for treatment of long-lasting conditions such as cancer and chronic pain which require controlled, localized, and sustained drug release.

Keywords

piroxicam; drug release mechanism; drug-loaded nanoparticles; hydrogel; localized delivery

Introduction

One of the main challenges in drug delivery is to ensure localized and controlled release of drugs to minimize side effects and increase drug efficacy. This control can be attained by using so called “smart materials” that respond to an external stimulus, thereby releasing their payload. Several drug delivery systems (DDSs) have been developed that release drugs caused by pH change [1,2], magnetic field [3–5], enzymes [6,7], oxidation/reduction [8,9], light [10], temperature [11], ultrasound [12,13] and electrical stimuli [14–17]. Out of these, one of the heavily investigated release system depends on pH change as it does not require any external stimulus. The inherent pH in different parts of the body vary, but remain locally rather constant. For example, the pH varies widely in different parts of the gastrointestinal tract: pH 1-3 in the stomach, pH 5 in the small intestine and pH 7-8 in the colon [2]. Sites of inflammation, bacterial infections or tumors have also been found to be more acidic (~pH 5-6.5) than physiological pH (~pH 7.4) [18–20].

The use of nanoparticles (NPs) in devising pH-based DDSs is appealing because of several reasons. NPs have a large surface-to-volume ratio, and therefore, the amount of drug that can be loaded in them is increased. Owing to their small size, they can be circulated in the body without causing any blockage, and delivered through the lymphatic system [21]. NPs also facilitate delivery

of hydrophobic and poorly bioavailable drugs [22], and can protect drugs from degradation until they reach their target site [23,24].

Most pH-sensitive drug carriers are based on polyelectrolytes with acidic (carboxylic acids, sulfonic acids, phosphoric acids) or basic (amines) ionizable moieties [25,26]. These groups can either accept or release protons, thereby causing conformation changes that lead to drug release. Carriers containing acid-cleavable bonds [27,28] are also common. Some examples of pH responsive systems include DDSs based on pH-sensitive micelles [29], liposomes [30], hydrogels [31], peptides [32], and hybrid organic-inorganic nanostructures [33]. Most of these systems can only release drugs above or below a certain pH. That is, there is no universal system that can selectively release drugs both at high and low pH, on a case by case basis. In this paper, we report the investigation of polypyrrole nanoparticles (PPy NPs) for devising such a versatile DDS.

PPy is an electrically conducting polymer which is both biocompatible and nontoxic [34,35]. It has been studied in detail for developing DDSs based on electrical stimulation [14–17,36,37]. However, the pH-sensitive behavior of PPy has received less attention for the purposes of drug delivery. Recently, Wang *et al.* [38] have shown that hollow PPy nanocapsules loaded with antitumor agent doxorubicin (DOX) are pH-sensitive, and release more than half of the encapsulated drug within 15 h at a pH of 4.5. They have also shown that the amount of release can be further increased by applying near infrared light. Park *et al.* [39] have studied PPy nanoparticles doped with hyaluronic acid for preferential release of DOX at lysosomal pH (pH<5). The mechanism of drug release from PPy NPs has not yet been investigated in detail.

In this work, we have synthesized polypyrrole nanoparticles (PPy NPs) without the use of dopants. We have loaded these PPy NPs with fluorescein sodium salt (FL), a negatively charged model drug, and rhodamine 6G (R6G), a positively charged model drug. We have studied the release characteristics of these two systems to understand the general mechanism of charged drug release from PPy NPs at desired pH. The pH responsiveness of our DDS can be used to take drugs orally. Also, these NPs can be delivered locally via a hydrogel in the treatment of diseases that need repeated doses such as chronic pain, cancer, diabetes, etc. To show this, we have studied piroxicam (PX), a nonsteroidal anti-inflammatory drug used in the treatment of rheumatoid arthritis. We have dispersed PX-loaded PPy NPs in a calcium alginate (CaAlg) hydrogel and monitored the sustained release of PX. Figure 1 presents a schematic of this drug delivery system. It should be noted that our system is not optimized for a particular drug. Instead, we explore the potential of PPy NPs for pH-sensitive and sustained drug delivery, with a focus on understanding the chief parameters that affect drug release.

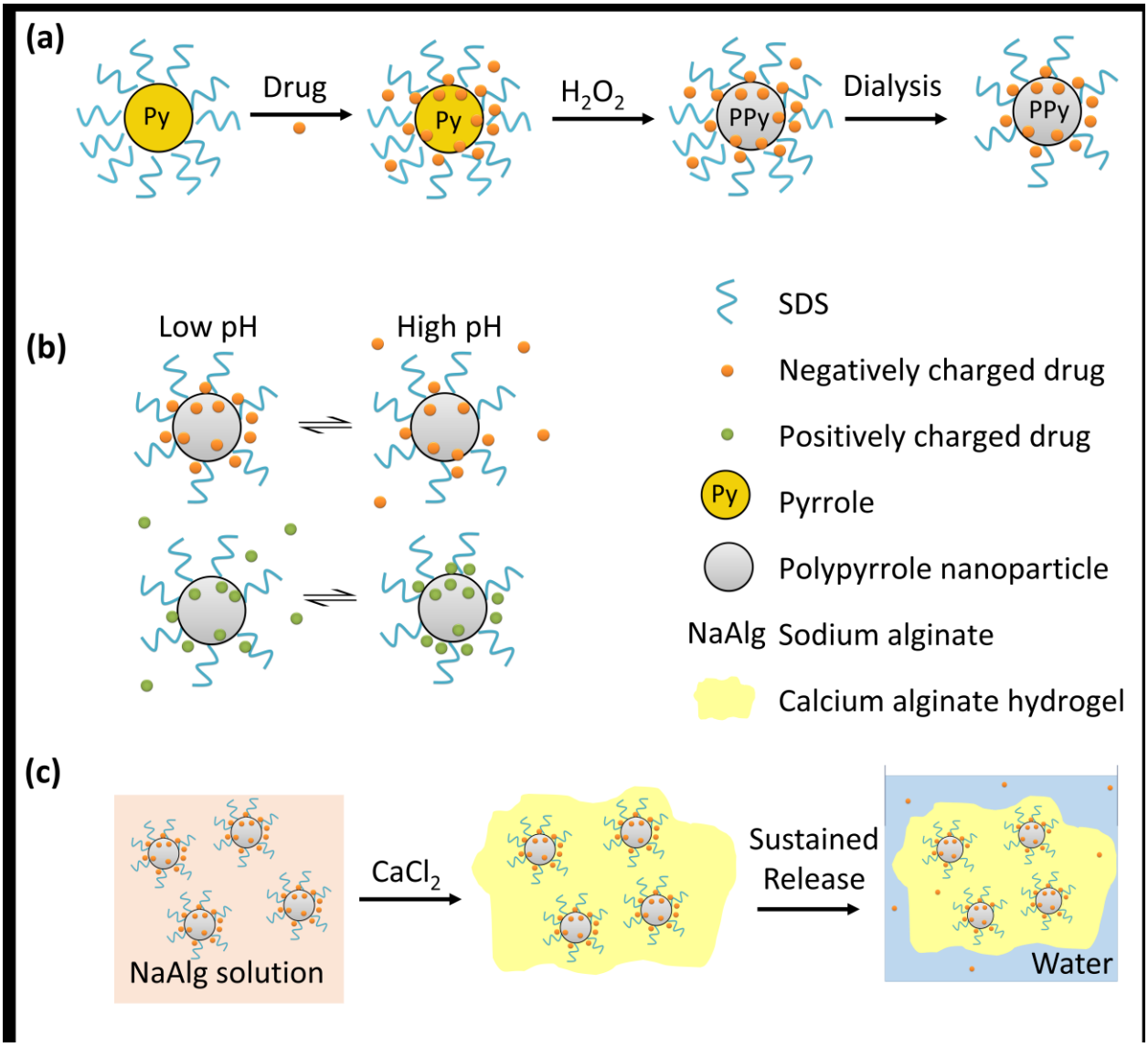

Figure 1. Schematic of the drug delivery system: (a) synthesis of the drug-loaded nanoparticles; (b) pH-triggered drug release; and (c) sustained release from a hydrogel containing embedded drug-loaded nanoparticles.

Materials

Pyrrole (reagent grade, 98%), sodium dodecyl sulfate (ReagentPlus®, ≥98.5%), 35 wt% hydrogen peroxide H_2O_2, piroxicam (>98%), fluorescein sodium salt, Trizma® hydrochloride buffer solution, TRIS-HCl buffer solution, Pur-A-Lyzer™ Dialysis Kits, Whatman® Anotop® 25 syringe filters, alginic acid sodium salt, calcium chloride (ReagentPlus®, 99.99%), and BD Falcon cell strainer (40 µm, Nylon) were purchased from Sigma Aldrich. Rhodamine 6G was purchased from Lambda Physik.

Methods

Synthesis of drug-loaded polypyrrole nanoparticles. All reactions and measurements were carried out in triplicate and at room temperature unless mentioned otherwise. In a typical synthesis, 144.2 mg of SDS were dissolved in 5 mL of 40 mM HCl solution. To this, 15 mg of the drug FL, PX or R6G were added and stirred with heating, if necessary, till complete dissolution. Then 100 µL pyrrole were added, followed by 200 µL 35 wt% hydrogen peroxide (H_2O_2). The solution started to darken immediately and turned black within 10 min after the addition of H_2O_2. The solution was stirred for 24 h to ensure complete yield of drug-loaded polypyrrole nanoparticles.

Washing the nanoparticles. 3 mL of the reaction mixture were washed using dialysis tubes (MWCO 3.5 kDa). The unwashed nanoparticles were placed in the dialysis tubes and the tubes were then immersed in 150 mL water (supernatant). The water was stirred for 24 h. The washed nanoparticles were transferred to a 15 mL centrifuge tube and the volume was adjusted to 6 mL with water. These nanoparticles were then stored under ambient conditions.

Calculation of drug loading. The drug loading was determined from the supernatant of the washing using the method of standard addition. 200 µL of the supernatant were placed in a Greiner flat-bottomed 96 well-plate. The well plate was read using a TECAN infinite M1000 plate reader. The UV-Vis spectrum was monitored between 250-500 nm for PX and 400-700 nm for FL and R6G, and readings were taken by adding 0, 10, 20, 30 and 40 µL of 50 µg/mL standard solution of the compound in water. The absorbance maxima were plotted as a function of the concentration of the added standard drug/drug model. The data points were fit by least squares to a straight line, and the x-intercept of the regression line gave the initial concentration of the drug/drug model in the wash.

Size and stability measurements. The size distribution of the nanoparticles was measured both before and after washing using dynamic light scattering (DLS) using a Malvern Zetasizer Nano ZS90 instrument. The washed nanoparticles were also imaged using scanning electron microscopy (SEM). For DLS, 5 µL of the washed nanoparticles were diluted with 2 mL of water and vortexed. The DLS reading was taken using 1 mL of the resultant solution. The number of measurements was set to 15. For SEM, 20 µL of the washed solution were placed on an aluminum SEM stub and dried overnight in a vacuum desiccator. The sample was then sputter coated, and the images were recorded with a Zeiss Sigma FESEM instrument.

To measure the stability of the nanoparticles, the size distribution of the nanoparticles was monitored over a period of 28 days using DLS. The zeta potential was also measured during that period of time by taking 10 µL of the nanoparticles and diluting them with 1 mL water. We found that the nanoparticles are essentially unchanged when stored at room temperature for a period of three months.

pH-triggered release. 80 µL of the washed nanoparticles and 80 µL of water were added to a 2 mL centrifuge tube. 1.44 mL of solution of appropriate pH were added to make a total volume of 1.6 mL. The solutions of different pH used were 0.01 M HCl (pH 2), 10^{-5} M HCl (pH 5), Trizma® hydrochloride buffer solution (pH 7.4), and 0.01 M TRIS-HCl (pH 8.0). Additionally, 1 M HCl, 2 M HCl and 3 M HCl solutions were used for R6G. Each resultant solution was

vortexed for 10 s and filtered through 0.02 μm syringe filters. The R6G filtrate from 1 M HCl, 2 M HCl and 3 M HCl solutions were neutralized by adding NaOH. To measure the effect of surfactant concentration at a fixed pH (7.4), a similar procedure was followed. In this case, instead of 80 μL of water, 16 μL and 32 μL of 100 mM SDS/DTAB were added to yield solutions with a final surfactant concentration of 1 mM and 2 mM in SDS/DTAB, respectively. The total volume was adjusted to 1.6 mL with water.

150 μL of the filtrate (100 μL for FL) were placed in each of 4 wells in a 96-well plate. 0, 10, 20, 30 μL of 50 μg/mL standard drug solution (5 μg/mL used for R6G) in water were added to the 4 wells respectively. The total volume was adjusted to 180 μL (130 μL for FL). The UV-Vis spectrum was recorded between 250-500 nm for PX and 400-700 nm for FL and R6G. The concentration of the drug in solution was found out using the method of standard addition as described above.

Sustained Release of PX. 750 μL of the PX-PPy NPs were dispersed in equal volume of 1% sodium alginate solution. The NP-alginate mixture was added to a cell strainer with 40 μm pores while it was soaked in 0.5 M calcium chloride. The calcium alginate (CaAlg) gel formed immediately as the alginate came into contact with Ca^{2+} ions. The cell strainer was then washed twice with 5 mL of water and placed in a 20 oz. glass vial. 10 mL of distilled water and a magnetic stir bar were added to this. The solution was replaced every day and the study was continued for 3 weeks. The absorbance of the solution was monitored every day. This experiment was replicated 5 times. The purpose of the cell strainer was to contain the hydrogel in place so that the spinning stir bar did not disintegrate the gel on impact. The pores were sufficiently high to allow free diffusion across the cell strainer. As a control, to prove that the release of PX is slowed primarily by the PPy NPs and not by the hydrogel, the experiment was repeated with the same amount of free PX as in the PPy NPs, dispersed in a bare CaAlg hydrogel.

Results and Discussion

Synthesis of Stable Polypyrrole Nanoparticles. The polypyrrole nanoparticles (PPy NPs) were synthesized by oxidative polymerization of pyrrole in an acidic micellar solution of sodium dodecyl sulfate (SDS). In 0.04 M HCl solution, SDS was dissolved to reach a concentration of 0.1 M (critical micellar concentration, CMC, of SDS in this environment is 3.3 mM [40]), followed by the dissolution of the compounds FL, PX and R6G, and pyrrole. The oxidation of pyrrole was initiated by the addition of H_2O_2. The mechanism of PPy formation using this synthetic route has been studied and is reported in literature [40]. Most chemical syntheses of PPy involve strong oxidizing agents such as ferric chloride, potassium dichromate, ammonium persulfate, potassium permanganate, etc. which leave traces of these toxic materials embedded into the polymer matrix [40,41]. The use of H_2O_2 avoids these complications and is, therefore, more suitable for biomedical applications. Moreover, we chose this synthesis route as other methods do not give such small nanoparticles [36], and the nanoparticles tend to aggregate over time, attested by discrepancies between the size measured using DLS and that measured by SEM [36].

After 24 h of stirring, the nanoparticles were dialyzed for another 24 h in water to remove impurities and loosely bound drug molecules. The loading was calculated in terms of weight

percentage with respect to the amount of compound initially added as well as the amount of pyrrole initially added. Almost all of the compounds added was incorporated into PPy (99.9% for FL, 97.7% for PX, and 100% for R6G). By weight of pyrrole, the loading was ~15% for each compound. This is about a four-fold increase in loading capacity compared to that of FL-loaded PPy NPs synthesized by another chemical method reported before [36]. This figure might also be compared with that achieved by Park *et al*. [39] who reported a 6.5% loading of doxorubicin onto PPy NPs doped with hyaluronic acid.

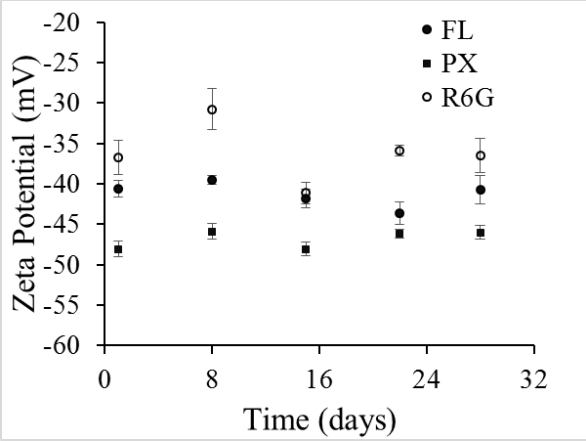

Figure 2. Zeta potential of PPy NPs. Uncertainties are one standard deviation (3 measurements).

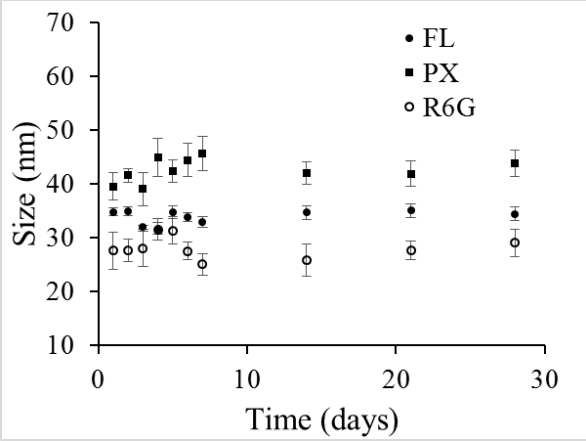

Figure 3. Sizes of PPy NPs measured by DLS. Uncertainties are one standard deviation (3 measurements).

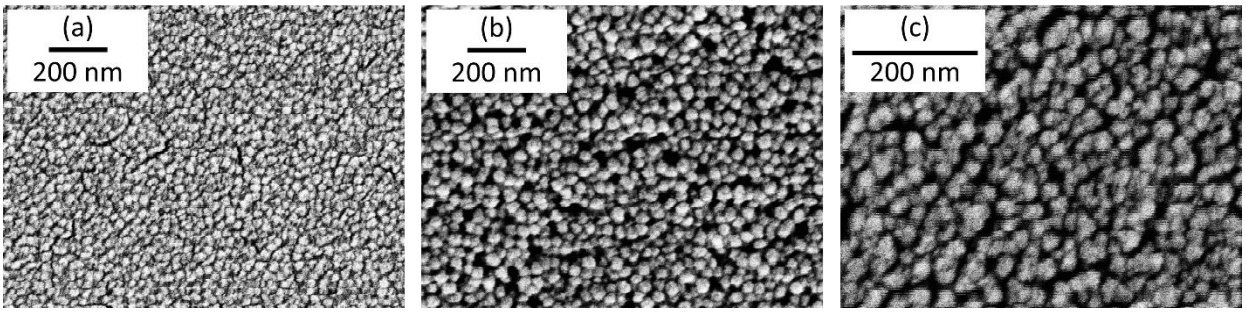

Figure 4. SEM images of (a) FL-PPy, (b) PX-PPy, and (c) R6G-PPy.

As a measure of stability, the zeta potential and the size of the nanoparticles were monitored over the period of a month. The purpose of this study was to ensure that the nanoparticles can be stored in solution, bypassing the need for drying and redispersing them. It is assumed that as long as the drug is attached to the PPy, it will not degrade [42]. PPy NPs are known to have a positively charged backbone resulting from overoxidation. [40] Figure 2 shows the zeta potential of the PPy NPs. For all compounds, irrespective of their charges, the surface charge of the nanoparticles is negative and less than -30 mV. This fact can be understood by realizing that the adsorption of excess negatively charged SDS molecules gives the nanoparticles an overall negative charge. As expected, the zeta potential is less negative when a positively charged compound (R6G) is loaded. The strongly negative zeta potential suggests that the particles should not aggregate over time. This expected behavior is verified by size measurements (Figure 3) performed by DLS. The average DLS size of the nanoparticles is about 34 nm, 43 nm and 28 nm for FL-, PX- and R6G-loaded PPy, respectively. These results are consistent with SEM images of these nanoparticles (Figure 4). Both zeta potential and size are fairly constant over time, attesting to the inherent stability of these nanoparticles.

Tuning pH-Sensitive Drug Release. The release of the compounds from the PPy NPs was tested *in vitro* at four different biologically relevant pH, namely, pH 2, pH 5, pH 7.4, and pH 8. For this purpose, a small amount of the PPyNPs was added to a solution of the appropriate pH. The mixture was vortexed and the PPy NPs were removed by filtration. The amount of compound in the filtrate was monitored using UV-Vis spectroscopy. The absorption profiles of all the molecules studied here are sensitive to their environment. For example, the absorption maxima for FL shifts to shorter wavelengths at lower pH. The molar extinction coefficient also decreases [43,44]. Similarly, the absorbance of PX and R6G also depend on the surrounding media [45]. Therefore, to account for matrix effects, a standard addition method was employed to quantify the release.

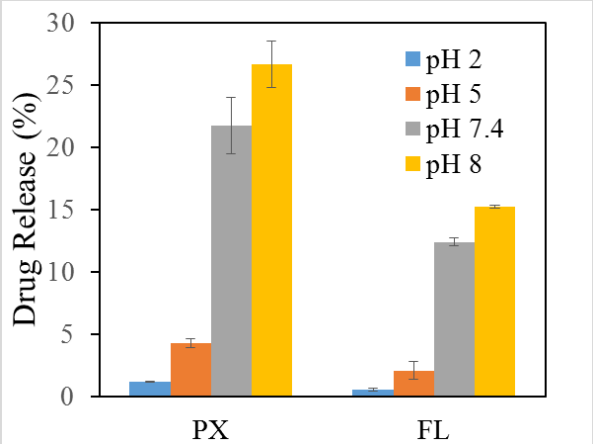

Figure 5. Release of FL and PX from PPy NPs. Uncertainties are one standard deviation (3 measurements).

We observed that for FL, which is a negatively charged model drug, increase in pH increases drug release (Figure 5). Intuitively, we expected the reverse to be true in case of R6G, which is positively charged. However, we could not detect any absorbance peak for R6G at the different biological pH tested. We hypothesized that it is possible that as lower pH should favor R6G release, environment more acidic than pH 2 might be necessary. To test our hypothesis, we tried three more release media: 1 M HCl, 2 M HCl, and 3 M HCl. As shown in Figure 6, the release of R6G increases with increasing acidity of the solution. Like FL, PX is also negatively charged, and its release behavior is analogous to that of FL (Figure 5). Please note that the data presented in Figs. 5 and 6 represent the percentage release of the drug after only 10 s of vortexing the nanoparticles in the relevant pH solutions. Higher release percentages are expected to occur from the nanoparticles when more equilibration time is allowed or under sink conditions. Given that our system is not optimized for any particular drug, the trends in drug release are more important than their exact magnitudes.

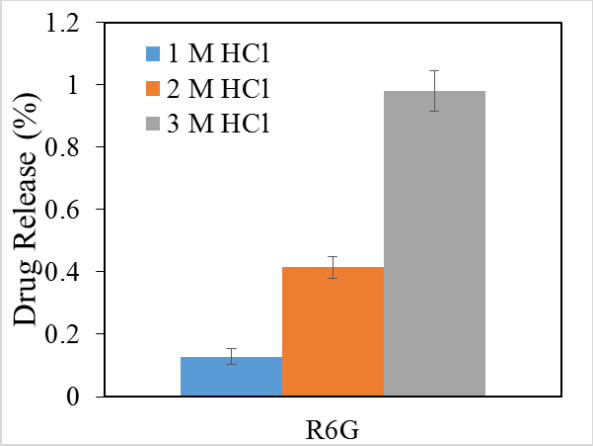

Figure 6. Release R6G from PPy NPs. Uncertainties are one standard deviation (3 measurements).

Mechanism of pH-Triggered Drug Release. The reported protonation pKa of PPy is 2-4 [46], and as prepared, PPy is partially protonated [40,46]. A more detailed mechanism of protonation and deprotonation of PPy can be found elsewhere [46,47]. In our case, the more acidic the pH, the more the protonation of PPy, and hence, more negatively charged compound can be associated with it. Higher pH favors more deprotonation of PPy and lowers the overall positive charge. This seems to facilitate the release of negatively charged drug cargo. In case of a positively charged drug, lower pH increases the net positive charge on the PPy backbone and therefore causes electrostatic repulsion that pushes out the drug. The strong binding of positively charged R6G to the positively charged PPy suggests that both electrostatic and hydrophobic interactions are involved in the interaction between compound and PPy. It is reasonable to believe that the adsorbed SDS on the surface of PPy also plays an important role in both compound attachment and detachment from PPy. It probably helps to mitigate same charge repulsions between PPy and R6G.

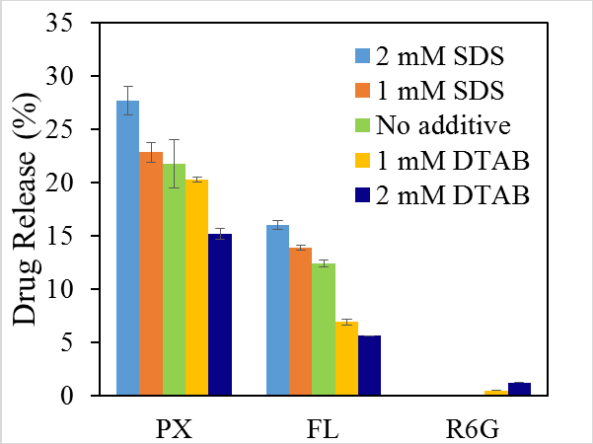

Figure 7. Effect of surfactants at different concentrations on drug release at constant pH (7.4). Uncertainties are one standard deviation (3 measurements).

If pH were the only parameter that governs drug release, this PPy-based DDS may not be appropriate for delivering positively charged drugs, because like R6G, other positive drugs would also possibly bind too strongly to the NPs. Given that the release mechanism arises from changes in surface charge, the addition of small amounts of surfactants should also modify the release.

From Figure 7, we can clearly see this variation in release when SDS and dodecyltrimethylammonium bromide (DTAB) are added at a constant pH of 7.4. SDS, being negatively charged, increases release of FL and PX. On the contrary, DTAB, being positively charged, decreases their release. In contrast, DTAB increases the release of R6G. The amount of release scales with the amount of surfactant added. This behavior is probably because the additional surfactants attach or move to the surface of the NPs. In case of similarly charged compounds, the surfactants compete with binding and push out more of the compound. Compounds of opposite charge are held more strongly electrostatically. In our study we have employed 1 mM and 2 mM surfactant concentrations which are below the CMC of both surfactants. Above the CMC, different surfactants can aggregate differently [48,49], and the release under those circumstances would be more complicated.

Encapsulation in a Hydrogel for Sustained Release. For testing local delivery of the PPy NPs, we dispersed the PX-PPy NPs in a calcium alginate (CaAlg) hydrogel. PX is a hydrophobic pain medication with poor bioavailability. Given that the half-life of this drug is about 30 h [50], it would be beneficial to have this compound delivered in an extended manner, particularly for patients with chronic pain. The hydrogel was prepared by the addition of sodium alginate solution containing the PPy NPs to a solution of calcium chloride. Contact between these two solutions immediately leads to the formation of the gel, as the Ca^{2+} ions start cross-linking the alginate molecules. The release of PX was monitored over the period of three weeks (Figure 8). We observed that the release is very slow, and only ~19% of the incorporated PX is released in this time. In comparison, the majority of existing sustained release formulations of PX release a significant portion of the encapsulated drug (between 60-80%) within a few hours [51,52]. Without the PPy NPs, 94% of the same amount of PX dispersed in bare CaAlg hydrogel is released within 5 days (Figure 9). Our results show that the diffusion of PX is inhibited primarily by the PPy NPs, and not the hydrogel. It should be mentioned that the release can also be modified by varying the proportions of Ca^{2+} ions and alginate [53]. Elevated concentrations of Ca^{2+} ions increase the cross-linking of the hydrogel, and therefore, decelerate the release [53].

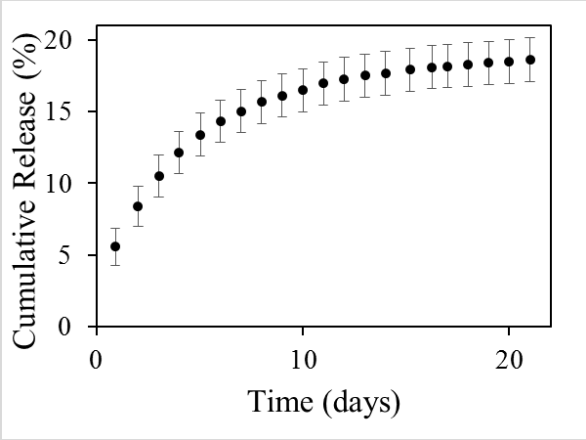

Figure 8. Sustained release of PX from PPy NPs. Uncertainties are one standard deviation (5 measurements).

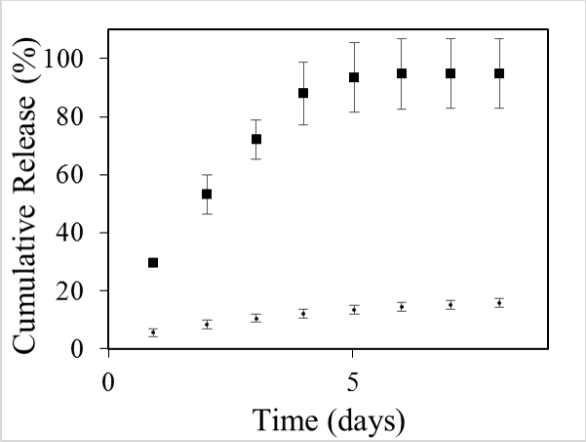

Figure 9. Comparison between PX release from bare CaAlg hydrogel (solid squares) and from PPy NPs dispersed in CaAlg (solid dots). Uncertainties are one standard deviation (3 measurements for bare hydrogel and 5 measurements for PX-PPy NPs in hydrogel).

Conclusions

We have synthesized stable, monodisperse PPy NPs with a drug loading capacity as much as 15% by weight, and showed that these NPs can be used as a versatile drug delivery platform for releasing both positively and negatively charged drugs. The drug release can be triggered by a change in pH and can be fine-tuned by addition of small amounts of surfactant to the NPs. In general, negatively charged drugs are released more at higher pH and positively charged drugs are released more at lower pH. This system might be particularly important in the treatment of cancer, given that anti-cancer drugs of the anthracycline family such as doxorubicin, daunorubicin, etc. are positively charged [36,39], and would be preferentially released in more acidic cancerous tissue. Other diseases that either occur in parts of the body that have a pH different from the physiological pH or cause the local pH to change from 7.4 can also benefit from such a DDS. Moreover, these nanoparticles are promising as sustained release vehicles.

Acknowledgements

We would like to thank Lydia-Marie Joubert at The Cell Sciences Imaging Facility (CSIF), Stanford University, for helping us with the SEM imaging. We also acknowledge the Center for Molecular Analysis and Design (CMAD), Stanford University, and the German Academic Exchange Service (DAAD), Germany, for funding.

References

1 W. Chen, P. Zhong, F. Meng, R. Cheng, C. Deng, J. Feijen and Z. Zhong, *J. Control. Release*, 2013, **169**, 171–179.

2 V. Balamuralidhara, T. M. Pramodkumar, N. Srujana, M.P. Venkatesh, V. Gupta, K. L. Krishna, H. V. Gangadharappa, *Am. J. Drug Discov.* 2011, **1**, 24–48.

3 H. Oliveira, E. Pérez-Andrés, J. Thevenot, O. Sandre, E. Berra and S. Lecommandoux, *J. Control. Release*, 2013, **169**, 165–170.

4 C. Sun, J. S. H. Lee and M. Zhang, *Adv. Drug Deliv. Rev.*, 2008, **60**, 1252–1265.

5 C. Fang, F. M. Kievit, O. Veiseh, Z. R. Stephen, T. Wang, D. Lee, R. G. Ellenbogen and M. Zhang, *J. Control. Release*, 2012, **162**, 233–241.

6 M. A. Azagarsamy, P. Sokkalingam and S. Thayumanavan, *J. Am. Chem. Soc.*, 2009, **131**, 14184–14185.

7 P. D. Thornton and A. Heise, *J. Am. Chem. Soc.*, 2010, **132**, 2024–2028.

8 Y. Jiao, Y. Sun, B. Chang, D. Lu and W. Yang, *Chem. Eur. J.*, 2013, **19**, 15410–15420.

9 M. Cai, K. Zhu, Y. Qiu, X. Liu, Y. Chen and X. Luo, *Colloids Surf. B: Biointerfaces*, 2014, **116**, 424–431.

10 V. Shanmugam, S. Selvakumar and C.S. Yeh, *Chem. Soc. Rev.*, 2014, 6254-6287.

11 D. Needham and M. W. Dewhirst, *Adv. Drug Deliv. Rev.*, 2001, **53**, 285–305.

12 K. W. Ferrara, *Adv. Drug Deliv. Rev.*, 2008, **60**, 1097–1102.

13 J. Di, J. Price, X. Gu, X. Jiang, Y. Jing and Z. Gu, *Adv. Healthc. Mater.*, 2014, **3**, 811–816.

14 R. Wadhwa, C. F. Lagenaur and X. T. Cui, *J. Control. Release*, 2006, **110**, 531–541.

15 X. Luo and X. T. Cui, *Electrochem. commun.*, 2009, **11**, 402–404.

16 K. Kontturi, P. Pentti and G. Sundholm, *J. Electroanal. Chem.*, 1998, **453**, 231–238.

17 G. Jeon, S. Y. Yang, J. Byun and J. K. Kim, *Nano Lett.*, 2011, **11**, 1284–1288.

18 K. Engin, D. B. Leeper, J. R. Cater, a J. Thistlethwaite, L. Tupchong and J. D. McFarlane, *Int. J. Hyperthermia*, 1995, **11**, 211–6.

19 R. J. Gillies, in *Trends in Molecular Medicine*, 2001, vol. 7, pp. 47–49.

20 J. Liu, Y. Huang, A. Kumar, A. Tan, S. Jin, A. Mozhi and X.J. Liang, *Biotechnol. Adv.*, 2013, **32**, 693–710.

21 Y. Nishioka and H. Yoshino, *Adv. Drug Deliv. Rev.*, 2001, **47**, 55–64.

22 Y. S.R. Krishnaiah, *J. Bioequiv. Availab.*, 2010, **02**, 28–36.

23 R. H. Muller and C. M. Keck, *J. Biotechnol.*, 2004, **113**, 151–170.

24 J. Lu, M. Liong, J. I. Zink and F. Tamanoi, *Small*, 2007, **3**, 1341–1346.

25 X. Gu, J. Wang, Y. Wang, Y. Wang, H. Gao and G. Wu, *Colloids Surf. B: Biointerfaces*, 2013, **108**, 205–211.

26 E. S. Lee, K. Na and Y. H. Bae, *J. Control. Release*, 2005, **103**, 405–418.

27 Y. Bae and K. Kataoka, *Adv. Drug Deliv. Rev.*, 2009, 61, 768–784.

28 Y. Bae, S. Fukushima, A. Harada and K. Kataoka, *Angew. Chemie - Int. Ed.*, 2003, **42**, 4640–4643.

29 E. S. Lee, K. Na and Y. H. Bae, *J. Control. Release*, 2003, **91**, 103–113.

30 M. Zignani, D. C. Drummond, O. Meyer, K. Hong and J. C. Leroux, *Biochim. Biophys. Acta - Biomembr.*, 2000, **1463**, 383–394.

31 Y. Yue, X. Sheng and P. Wang, *Eur. Polym. J.*, 2009, **45**, 309–315.

32 O. A. Andreev, D. M. Engelman and Y. K. Reshetnyak, *Mol. Membr. Biol.*, 2010, **27**, 341–352.

33 S. Guo, Y. Huang, Q. Jiang, Y. Sun, L. Deng, Z. Liang, Q. Du, J. Xing, Y. Zhao, P. C. Wang, A. Dong and X. J. Liang, *ACS Nano*, 2010, **4**, 5505–5511.

34 M. Mattioli-Belmonte, F. Gabbanelli, M. Marcaccio, F. Giantomassi, R. Tarsi, D. Natali, A. Callegari, F. Paolucci and G. Biagini, *Mater. Sci. Eng. C*, 2005, **25**, 43–49.

35 D. D. Ateh, H. A. Navsaria and P. Vadgama, *J. R. Soc. Interface*, 2006, **3**, 741–752.

36 J. Ge, E. Neofytou, T. J. Cahill, R. E. Beygui and R. N. Zare, *ACS Nano*, 2012, **6**, 227–233.

37 L. L. Miller, B. Zinger and Q. Zhou, 1987, 2267–2272.

38 Y. Wang, Y. Xiao and R. Tang, *Chem. - A Eur. J.*, 2014, **20**, 11826–11834.

39 D. Park, Y. Cho, S.-H. Goh and Y. Choi, *Chem. Commun.*, 2014, **50**, 15014–15017.

40 K. Leonavicius, A. Ramanaviciene and A. Ramanavicius, *Langmuir*, 2011, **27**, 10970–10976.

41 S. P. Armes, *Synth. Met.*, 1987, **20**, 365–371.

42 S. Mura, J. Nicolas and P. Couvreur, *Nat. Mater.*, 2013, **12**, 991–1003.

43 N. Klonis and W. Sawyer, *Photochem. Photobiol.*, 2000, **72**, 179–85.

44 R. Sjöback, J. Nygren and M. Kubista, *Spectrochim. acta. Part A, Mol. Biomol. Spectrosc. Mol. Biomol. Spectrosc.*, 1995, **51**, L7–L21.

45 F. L. Arbeloa, I. L. Gonzalez, P. R. Ojeda and I. L. Arbeloa, *J. Chem. Soc. Faraday Trans. 2*, 1982, **78**, 989.

46 Q. Pei and R. Qian, *Synth. Met.*, 1991, **45**, 35–48.

47 M. Forsyth and V. T. Truong, *Polymer*, 1995, **36**, 725–730.

48 A. R. Katritzky, L. M. Pacureanu, S. H. Slavov, D. A. Dobchev, D. O. Shah and M. Karelson, *Comput. Chem. Eng.*, 2009, **33**, 321–332.

49 E. D. Goddard, *Colloids and Surfaces*, 1989, **40**, 347.

50 M. Mihalić, H. Hofman, J. Kuftinec, B. Krile, V. Čaplar, F. Kajfež and N. Blažević, *Anal. Profiles Drug Subst.*, 1986, **15**, 509–531.

51 A. Sezer, *Int. J. Pharm.*, 1995, **121**, 113–116.

52 P. Del Gaudio, G. Auriemma, P. Russo, T. Mencherini, P. Campiglia, M. Stigliani and R. P. Aquino, *Eur. J. Pharm. Biopharm.*, 2014, **87**, 541–547.

53 N. Paradee, A. Sirivat, S. Niamlang and W. Prissanaroon-Ouajai, *J. Mater. Sci. Mater. Med.*, 2012, **23**, 999–1010.

Table of Contents Graphic

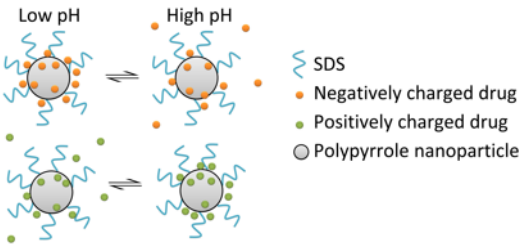

One sentence highlighting novelty of research results

Charged drug molecules from nanoparticles are released by changing the pH of the surroundings and fine-tuned by adding appropriate amphiphiles.